Gelatin and tannic acid based iongels for muscle activity recording and stimulation electrodes

Ana Aguzin[a], Gisela C. Luque[a,b], Ludmila I. Ronco[a,b], Isabel del Agua[c], Gregorio Guzmán-González[d], Bastien Marchiori[c], Agustina Gugliotta[e], Liliana C. Tomé[f], Luis M. Gugliotta[a,b], David Mecerreyes[d,g], and Roque J. Minari[a,b]**

[a] Instituto de Desarrollo Tecnológico para la Industria Química (INTEC), CONICET, Güemes 3450, Santa Fe 3000, Argentina.

[b] Facultad de Ingeniería Química, Universidad Nacional del Litoral, Santiago del Estero 2829, Santa Fe 3000, Argentina.

[c] Panaxium SAS, Aix-en-Provence 13100, France

[d] POLYMAT University of the Basque Country UPV/EHU, Joxe Mari Korta Center, Avda. Tolosa 72, 20018 Donostia-San Sebastian, Spain.

[e] UNL, CONICET, FBCB (School of Biochemistry and Biological Sciences), CBL (Biotechnological Center of Litoral), Ciudad Universitaria, Ruta Nacional 168 Km 472.4, C.C. 242. (S3000ZAA), Santa Fe, Argentina.

[f] LAQV-REQUIMTE, Department of Chemistry, NOVA School of Science and Technology, FCT NOVA, Universidade NOVA de Lisboa, 2829-516 Caparica, Portugal.

[g] Ikerbasque, Basque Foundation for Science, 48013 Bilbao, Spain.

Corresponding Authors:

Roque J. Minari: rjminari@santafe-conicet.gov.ar

David Mecerreyes: david.mecerreyes@ehu.es

Abstract

Iongels are soft ionic conducting materials, usually comprised of polymer networks swollen with ionic liquids (ILs), which are being investigated for applications ranging from energy to bioelectronics. The employment of iongels in bioelectronic devices such as bioelectrodes or body sensors has been limited by the lack of biocompatibility of the ILs and/or polymer matrices. In this work, we present iongels prepared from solely biocompatible materials: i) a biobased polymer network containing tannic acid as a crosslinker in a gelatin matrix, and ii) three different biocompatible cholinium carboxylate ionic liquids. The resulting iongels are flexible and elastic with Young's modulus between 11.3 and 28.9 kPa. The morphology of the iongels is based on a dual polymer network system formed by both chemical bonding due to the reaction of the gelatin's amines with the polyphenol units and physical interactions between the tannic acid and the gelatin. These biocompatible iongels presented high ionic conductivity values, from 0.003 and up to 0.015 $S*cm^{-1}$ at room temperature. Furthermore, they showed excellent performance as conducting gel in electrodes for electromyography recording as well as muscle stimulation.

Keywords

Iongels, Cholinium Carboxylate Ionic Liquids, Gelatin, Phenolics, Bioelectronics.

Introduction

Nowadays, ionic and electronic conducting polymers are actively being searched for the development of new bioelectronic devices such as Organic Electrochemical Transistors (OECTs), body and pressure sensors, electronic skin interfaces, mechanical actuators, biomimetic devices, supporting scaffolds, and ion pumps, among others.[1–7] Soft ionic conductors can be used as interfaces between electronic devices and biological tissue, by selectively allowing the ion flux.[8] The most commonly used materials as flexible bioelectrodes are hydrogels, due to their excellent adhesive properties, facile synthesis, high ionic conductivity and biocompatibility.[9] However, the main drawback of hydrogels is the loss of their properties over time as a consequence of water evaporation. Hydrogel-based devices in long-lasting experiments must undergo an extra step, comprising a sealing process to prevent dehydration.[10] As an alternative, iongels composed of non-volatile ionic liquids (ILs) instead of water have emerged as alternative soft-ionic conducting materials for long-lasting experiments.[8]

The variety of gelators that can constitute the 3D network of an iongel and the high number of ILs, implies a broad range of different combinations. In addition, iongels present good ionic conductivity, mechanical strength and flexibility allowing their application at high strains. Particularly in the biomedical field, iongels have been studied for applications such as artificial skin devices,[11,12] sensors,[10,13] and electrophysiology.[14–16] In this context, the development of new biocompatible iongel materials is of high interest given they are excellent candidates to fabricate devices which are in direct contact to the human body.

The application of iongels in the bioelectronic field has been limited by the absence of biocompatibility of conventional ILs and/or polymer matrices. The toxicity and the ecotoxicity of diverse ILs have been intensively studied.[16–18] In particular, the cholinium cation of the family of choline-based salts (a biodegradable compound with low toxicity) has been used to design biocompatible ILs combining amino acids or carboxylic acids as anions.[19] Moreover, iongels

made of cholinium carboxylate ILs have already shown great potential to be used for bioelectronic applications.[16,20,21]

Considering that the gelator is also required to be biocompatible, it is common to use biopolymers or bio-safe synthetic polymers for the formation of iongels, such as PVA,[22,23] cellulose,[16,24–27] or guar gum.[28] Gelatin has also been previously tested as a gelator of imidazolium-based ILs,[29] but the resulting iongels were found to have poor mechanical strength, especially at high concentrations of IL. One of the biggest challenges regarding the application of iongels is to gather together two contradictory requirements, which are high ionic conductivity (i.e., high IL concentration) and high mechanical strength. Note that biopolymers with large molecular weights are difficult to dissolve in ILs, making the two phases incompatible. Among the different biopolymer gelators, gelatin possess ionic functionalities.[30] Gelatin presents charged amino acid residues which facilitate the formation of different dynamic interactions allowing higher compatibility between gelatin and ILs.[10]

In order to improve its mechanical properties, gelatin can be crosslinked by a wide spectrum of different molecules,[31] but the toxicity of many of these compounds (such as formaldehyde or glyoxal) restricts their application in medical-related fields.[32–34] Alternatively, natural phenolic compounds (PhCs) are an attractive alternative. There is a vast variety of PhCs that interact with proteins and allow the preparation of improved gels.[35–37] Thus, PhCs have been employed in the synthesis of both hydrogels and iongels.[21,22] Among the PhCs, tannic acid (TA) has the ability to form multiple and strong interactions. When combining gelatin and TA, the side chains of the protein amino acid can interact with the hydroxyl groups and aromatic rings of the TA,[31] resulting in different interactions, namely hydrogen bonds, electrostatic attraction, Van der Waals forces, hydrophobic interactions, and covalent bonds.[38] Although the ability of TA to interact with gelatin has already been reported, to the best of our knowledge, this has not been explored for the formation of iongel materials.

In this work, we present the synthesis and characterization of iongels composed of a gelatin-tannic acid polymer network and cholinium carboxylate ILs. Taking advantage of the interaction that phenolic compounds can have with proteins, our goal here is to fabricate elastic iongels, solely based on biocompatible materials, with the potential to be used as soft-ionic conducting materials in bioelectronic devices. Rheological studies and structural characterizations were performed and the biocompatibility of the materials was evaluated by cytotoxicity assays. Furthermore, the ionic conductivity, mechanical and thermal properties of the iongels were investigated and their potential application for electromyography recordings and muscle stimulation was finally assessed.

Materials and Methods

Materials

Gelatin (PB Leiner, 235/30 bloom), tannic acid (TA, Biopack, ACS reagent), choline bicarbonate (Sigma Aldrich), acetic acid (Sigma Aldrich), glycolic acid (Sigma Aldrich), and lactic acid (Sigma Aldrich), sodium chloride (NaCl, Cicarelli), potassium chloride (KCl, Cicarelli), sodium phosphate dibasic dodecahydrate ($NA_2HPO_4.12H_2O$, Anedra), potassium phosphate (KH_2PO_4, Cicarelli), chloride acid (HCl, Anedra, 37 %), 0.5 % Trypsin-EDTA (10X, Gibco); CellTiter 96® AQueous One Solution Cell Proliferation Assay (MTS/PMS, Promega), Poly(3,4-ethylenedioxythiophene): poly(styrene sulfonate) (PEDOT:PSS) (Clevios PH1000, Heraeous), ethylene glycol (EG) (Sigma Aldrich), 4-dodecylbenzenesulfonic acid (DBSA) (Sigma Aldrich), 3-Glycidyloxypropyl (GOPS) (Sigma Aldrich) were used. Distilled-deionized water was used for all experiments. All chemical agents were employed as received, without further purification.

Synthesis of Cholinium-based Ionic Liquids

The cholinium-based ionic liquids used in this work were synthesized by dropwise addition of the corresponding acid (1:1) to aqueous choline bicarbonate, following an established procedure.[20] The resulting solution was stirred at room temperature for 12 h, and then washed with diethyl ether to remove the unreacted acid. Rotary evaporation and subsequently stirring and heating under vacuum at moderate temperature (40 – 50 °C) were carried out to remove the excess water and remaining traces of organic solvent. The chemical structures and the purities of the ILs were confirmed by ^{1}H-NMR.

Cholinium Acetate ([Ch][Ac]): ^{1}H NMR (400 MHz, D_2O): δ/ppm =1.75 (s, 3H, C**H**$_3$COO); 3.04 (s, 9H, N(C**H**$_3$)$_3$); 3.35 (t, 2H, NC**H**$_2$CH$_2$OH); 3.90 (m, 2H, NCH$_2$C**H**$_2$OH).

Cholinium Glycolate ([Ch][Gly]): ^{1}H NMR (400 MHz, D_2O): δ/ppm = 3.8 (d, 2H, COO(C**H**$_2$)OH); 3.07 (s, 9H, N(C**H**$_3$)$_3$); 3.4 (t, 2H, NC**H**$_2$CH$_2$OH); 3.93 (m, 2H, NCH$_2$C**H**$_2$OH).

Cholinium Lactate ([Ch][Lac]): ^{1}H NMR (400 MHz, D_2O): δ/ppm = 1.17 (d, 3H, OOCCH(C**H**$_3$)OH); 3.07 (s, 9H, N(C**H**$_3$)$_3$); 3.38 (t, 2H, NC**H**$_2$CH$_2$OH); 3.92 (m, 2H, NCH$_2$C**H**$_2$OH); 3.97 (q, 1H,OOC**H**(CH$_3$)OH).

Preparation of Iongels

All the iongels were prepared with 10 wt% of gelatin concentration, variable content of TA (5, 10, 20 wt% based on gelatin), and different ILs. The chemical structures of the iongel components are shown in Figure 1. Water was added as 50/50 LI-H_2O to guarantee the proper dissolution of all components. The procedure involved the dissolution of the components (gelatin, TA, LI, and water) in their corresponding quantities, under constant temperature (90 °C) and continuous stirring. For example, to prepare an iongel with [Ch][Ac] IL and 20 wt% of TA, 0.10 g of gelatin was dissolved at 90 °C in 0.5 g of water under vigorous stirring. Then, 0.5 g of [Ch][Ac] IL and 0.02 g of TA were added. After one hour of continuous stirring at the mentioned

temperature, the resulting solution was poured into silicone molds and left at room temperature until gelation.

The experiments were codified including the abbreviation of the IL employed and followed by the concentration of TA. Thus, the experiment IG-ChAc-TA_{10} corresponds to an iongel made of [Ch][Ac] IL and 10 % of TA.

Characterization methods

Attenuated total reflection Fourier transform infrared (ATR-FTIR) spectra were collected using a Nicolet Magna IR 550 Series II spectrometer, furnished with an MCT-A detector, from 1000 to 4000 cm^{-1}, with a resolution of 4 cm^{-1} after 24 scans.

Thermogravimetric analyses (TGA) were performed using Q500 equipment from TA Instruments. Approximately 5 mg of sample were heated at a constant rate of 10 °C/min, within the 20-400 °C range, under a controlled nitrogen atmosphere.

To determine the rheological behavior of iongels, dynamic thermomechanical analyses (DMTA) were carried out. Samples of approximately 1 mm of thickness were analyzed using a 50 mm compression clamp on a TA Instruments Q800 equipment, and two different analyses were performed: *i*) a frequency sweep between 1 and 100 Hz, at 35 °C; and *ii*) a temperature sweep from 35 to 120 °C at a constant heating rate of 3 °C/min at 1 Hz.

Compression and tensile tests were also performed on the iongel samples to study their mechanical behavior, at 23 °C and 50 % of relative humidity. An INSTRON 3344 universal tester equipped with a 10 N load cell was used. Iongels discs of 1 mm of thickness and 8 mm of diameter were subjected to compression tests, where a 10 mm diameter plane-tip moved down at a constant speed (0.016 mm/s) until deformation of approximately 40% in the height of the sample. The compression and recovery cycles were repeated 5 consecutive times in each sample, with a 30 s time waiting period between each cycle, as to give sufficient time for the

sample to relax. The tensile tests were performed using samples with a rectangular shape (of 10 mm in length), at a constant rate of 0.41 mm/s.

The microstructure of the iongels was studied by performing scanning electron microscopy (SEM) measurements on a LEO equipment, model EVO 40 XVP at 5 kV. The samples were metalized with gold (Au) in a PELCO 9100 sputter coater and then observed with different magnifications (at 100, 500, 1000, and 2000x).

The ionic conductivity was measured by electrochemical impedance spectroscopy (EIS); a schematic of the measurement cell can be found in Figure S1.a of the Supporting Information (SI). An Autolab 302N potentiostat-galvanostat was used coupled to a Microcell HC station to control the temperature during the measurements, and circular iongels samples of approximately 8 mm in diameter were used. The iongels were sandwiched between two electrodes made of stainless steel and sealed in the Microcell. The measurements were carried out from 20 to 60 °C with a step of 10 °C holding the temperature for 20 min before each temperature change to allow temperature equilibration. The frequency range was set from 1.10^5 to 1 Hz, and the amplitude was 10 mV.

The cytotoxicity of iongels was evaluated using mouse-derived fibroblasts NIH/3T3 (ATCC CRL-1658). The cells were grown at 37℃ with 5% CO_2 in Dulbecco's modified Eagle's medium (DMEM) supplemented with 10% (v/v) fetal bovine serum (FBS). NIH/3T3 cells were incubated with iongels extracts that were obtained by incubation of each sample in 1 mL of cell growth medium [DMEM with 10% fetal bovine serum (FBS)] for 48 h at 37 °C. NIH/3T3 cells were seeded at a density of 10^5 cells/ml in DMEM 10% FBS into flat 96-well plates using 100 µL as the final volume per well (1000 cells per well) and incubated at 37 °C and 5% of CO_2. After overnight adhesion, the supernatant was removed from the plates and replaced with 100 µL/well of different dilutions of the iongels extracts: 1, 1/10, 1/100, 1/1000, 1/10.000. Those dilutions represent 100%, 10%, 1%, 0.1%, 0.01% medium replacement by iongels extracts.

Dilutions were performed in a fresh medium and incubated for 48 h. Controls were performed using a cytotoxic material (synthetic styrene-butadiene rubber) and a non-cytotoxic material (Teflon).[39] Proliferation control was performed using cells incubated with a fresh medium. Samples were analyzed in duplicates and three independent plates were prepared. After 48 h of incubation, pictures of the cells were taken using an inverted microscope (Eclipse Ti-S, Nikon Instruments Inc). Also, proliferation was determined using a CellTiter 96TM AQueous Non-Radioactive Cell Proliferation Assay (Promega, MTS/PMS colorimetric assay). Absorbance was read at 492 nm and 690 nm using a microplate reader (MultiskanTM, Thermo Fisher Scientific). The relative viability (%) was calculated considering the proliferation control as 100%. The statistical analysis was assessed using a one-way ANOVA followed by Dunnet post-tests.

Electromyography (EMG) recording and stimulation, electrocardiogram (ECG) recording, and skin-impedance experiments.

To fabricate the electrodes for the electromyography (EMG) recording and stimulation experiments, a Kapton sheet (75 µm) was covered with Ti 10 nm and 200 nm of gold by evaporation (Alliance concept). The coated Kapton was then laser cut (LPKF protolaser S) with the desired shape (4 x 4 cm and 1 x 0.5 cm connection). A PEDOT:PSS/GOPS solution (containing 5 % v/v EG, 1 % v/v GOPS, and 50 µL of DBSA for each 10 mL of mixture) was prepared following the referenced method,[40] drop-casted and dried at 50 °C for 15 min and then at 140 °C for 45 min. Before drying, the iongels (prepared as previously described) were drop-casted on top of the electrodes at 90 °C. Then, the electrodes slowly reached room temperature and were used for recordings, both on quadriceps and biceps. A schematic of the EMG experiment can be found in Figure S1.b. The commercial 4 x 4 cm medical electrodes used were bought from Quirumed; they are made of a carbon layer and coated with a hydrogel. Additionally, electrodes for electrocardiogram (ECG) experiments were equally fabricated with a circular shape of 1 cm diameter.

Muscle stimulation was produced using a Boston Tech WE-122 Electrotherapy Unit equipment, employing a program that sends 380 µs pulses at a frequency of 104 Hz. Electrodes were placed on the quadriceps according to the instruction manual and the current was increased with 1 mA steps until reaching visual muscle contraction without being considered painful. EMGs and ECGs were recorded using a Sienna Ultimate device plugging the bottom electrode to the reference. The signal was recorded with a hardware notch filter and the plotted signal was filtered with EDF Viewer using notch Filters at 50, 100, and 150 Hz. Impedance measures were performed for two of the iongels and a control electrode. A Potentiostat Metrohm Autolab 128N was used. A medical electrode was plugged into the referenced and counter electrode.

Results and discussion

Iongels samples with different TA concentration were prepared using three cholinium carboxylate ILs, namely [Ch][Ac], [Ch][Gly] and [Ch][Lac]. The chemical structures of the iongel components are shown in Figure 1.a, as well as the expected resulting layout of the iongel formation. The mechanism of the covalent crosslinking reaction proposed is shown in Figure 2. Polyphenol-protein crosslinking reactions have been previously described.[38,41] The TA is initially oxidized to a quinone, later reoxidized, and binds a second polypeptide, resulting in a crosslink between the phenol and the gelatin.[41] As illustrated in Figure 1.a, the iongel material structure can present not only covalent bonds but also physical interactions. The [Ch][Ac] based iongels were produced with three different TA concentrations, while iongels incorporating [Ch][Gly] and [Ch][Lac], were synthesized using the extremes of TA concentrations (5 and 20 wt%).

The resulting iongels containing gelatin and TA were flexible and easy to manipulate. Pictures of all the iongels formed are shown in Figure 1.b. The iongels were prepared from biocompatible ingredients and the distinctive brown color is due to the formation of *ortho*-quinone species as a consequence of phenolic compound oxidation.[21] As expected, the iongels became darker when

increasing the amount of TA incorporated. Although the iongels with 0 % of TA (i.e., without any crosslinking promoter) are formed merely due to the gelation ability of gelatin, the resulting materials are very soft and difficult to manipulate.

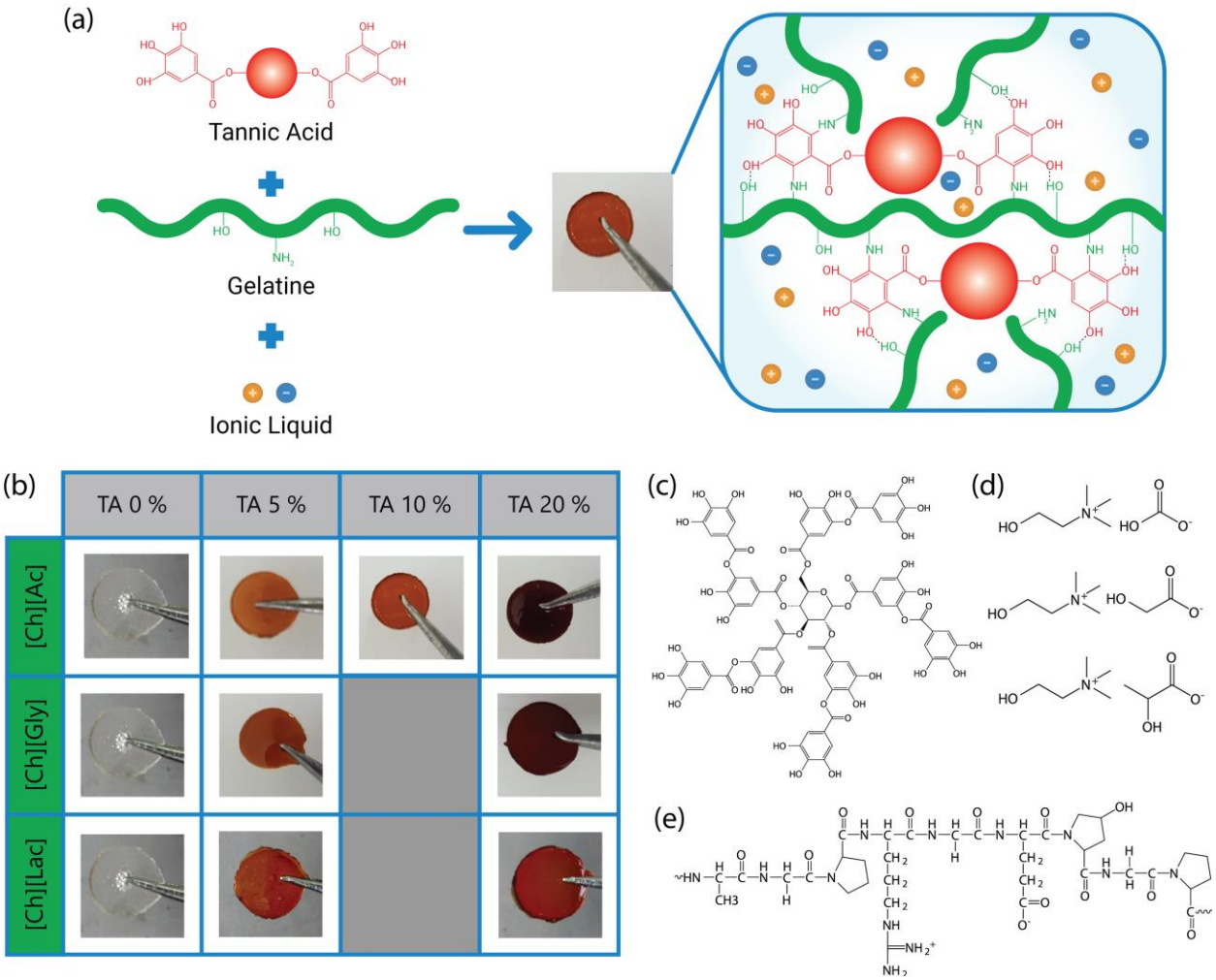

Figure 1. Schematic illustration of the iongels' formation, where gelatin is combined with TA and an IL (a), pictures of all the prepared iongels (b), chemical structure of tannic acid (TA) (c), ionic liquids (ILs) [Ch][Ac], [Ch][Gly] and [Ch][Lac] (d), and gelatin (e).

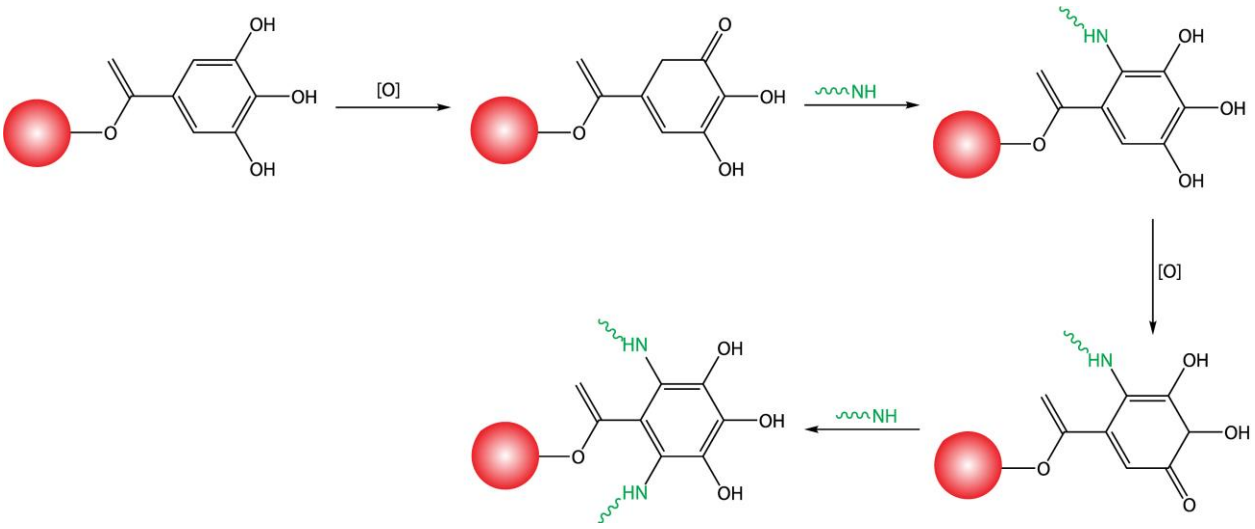

Figure 2. Reaction scheme of TA with the protein's amino groups.

To confirm the chemical structure of the iongels, all the samples were analyzed by ATR-FTIR. Figure 3 shows the spectra of the iongels containing [Ch][Gly] IL and variable TA content, including a sample without TA. No new peaks were identified among the different spectra, which is in agreement with what has previously been reported.[20,31,38,42] The main peaks detected through all the samples are the following: i) the band 3500-3000 cm^{-1} corresponding to the -OH and -NH stretching of both the primary and secondary amines (first enlargement); ii) the band 2990-2850 cm^{-1} corresponding to OH stretching (second enlargement), with the peak at 2960 cm^{-1} corresponding to the stretching vibrations of $-CH_2$; iii) the peaks at 1590 and 1641 cm^{-1}, corresponding to the -C=O and -OH stretching. In agreement with previous reports, the addition of TA into the system promoted shifts of the following peaks: a) the main peak at the band at 3500-3000 cm^{-1} shifted from 3276 cm^{-1} to 3261 cm^{-1} (attributed to a higher degree of binding between the -NH or -OH groups of the gelatin and the TA); and b) the peaks at 1590 and 1352 cm^{-1} shifted to 1585 and 1321 cm^{-1}, respectively (given by the structural changes in gelatin from helical to the random coil, and due to crosslinking).[31,42] These shifts are probably due to a chemical reaction between the TA and the gelatin. Similar shiftings of these peaks were observed for all the prepared iongels.

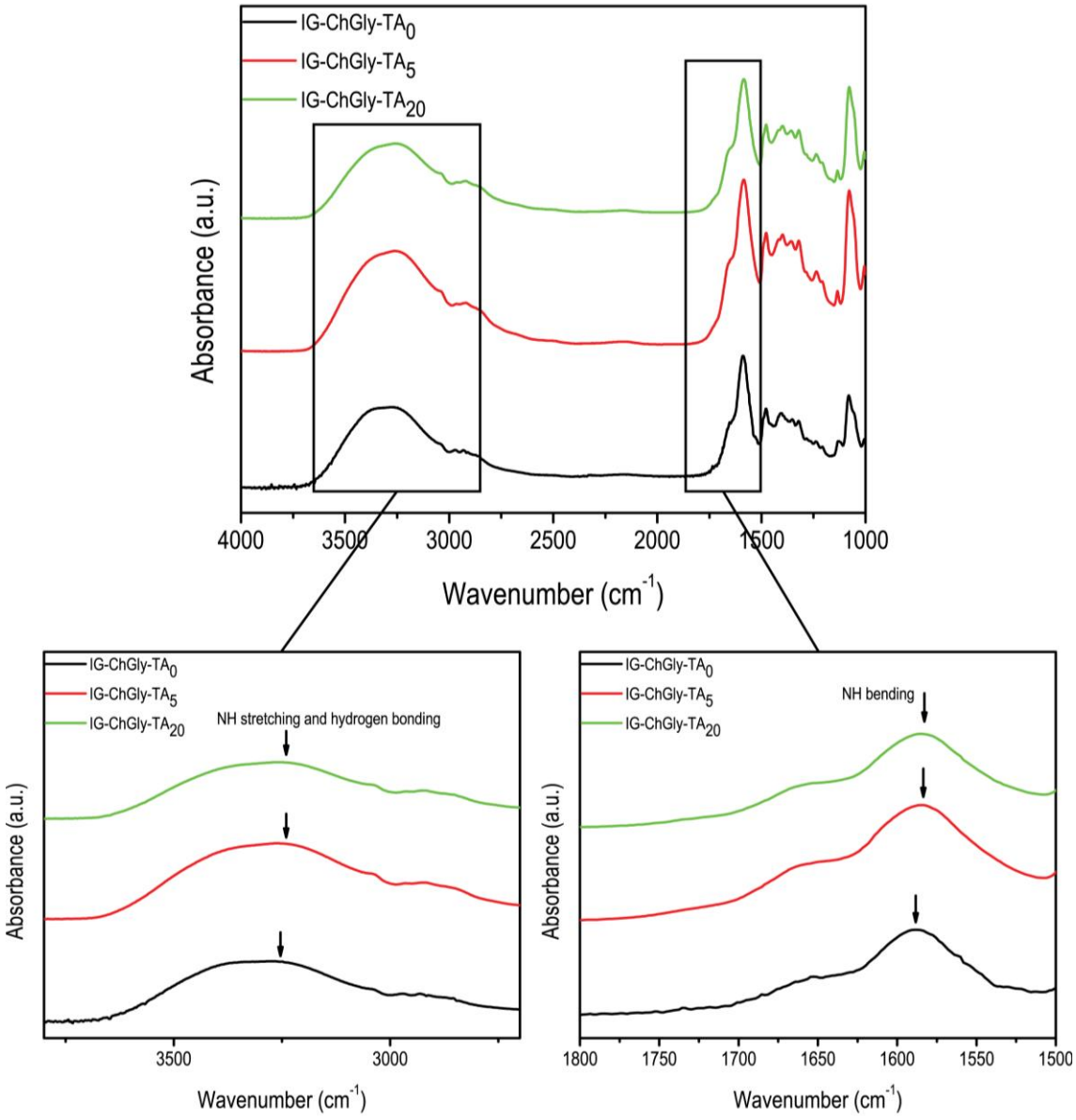

Figure 3. FTIR spectra of IG-ChGly with 0, 5, and 20 wt% of TA.

The dynamical rheological behavior of the iongels was studied by DMTA (Figure 4 and Figures S2-3 of SI). As can be seen in Figure 4 and Figure S2, the viscoelastic behavior as a function of the frequency shown by the iongels does not present a transition from an elastic network to a viscoelastic liquid in the frequency range studied (in the whole range, E' > E''). The same performance was also observed when studying the viscoelastic behavior as a function of the temperature (Figure S3). The stability of the iongel structure with the increase of both frequency and temperature corroborates the presence of a covalently crosslinked network. When

comparing the iongel samples formed with the same IL and increasing the TA content, a higher elastic modulus is observed. This probably indicates an increment of the crosslinking degree, which could be by both H bonding and covalent bonding. The iongels formed with [Ch][Ac] and 20 wt% of TA (IG-ChAc-TA_{20}) presented higher elastic modulus than their homologs containing [Ch][Gly] and [Ch][Lac], which is in agreement with previous reports.[20] When increasing the temperature (Figure S3), a small change in the storage modulus (E') occurred between 60 and 80 °C, without a moduli crossover. Even if small, this change in E' indicates that the iongels are probably formed by two different crosslinking mechanisms (covalent and hydrogen bonds gelatin-TA and gelatin-gelatin). At high temperatures, the structure remained a solid-like material due to the chemical links between gelatin and TA. Figures S3 and S5 of SI show that, in the absence of covalent bonds, the iongel (specially prepared in an atmosphere enriched with N_2 to avoid the reaction mechanism illustrated in Figure 2) presents a typical phase thermal transition (at 55 °C) of a supramolecular network. In the "Hybrid bonding" section of SI additional details and ad-hoc experiments were included to support this hypothesis.

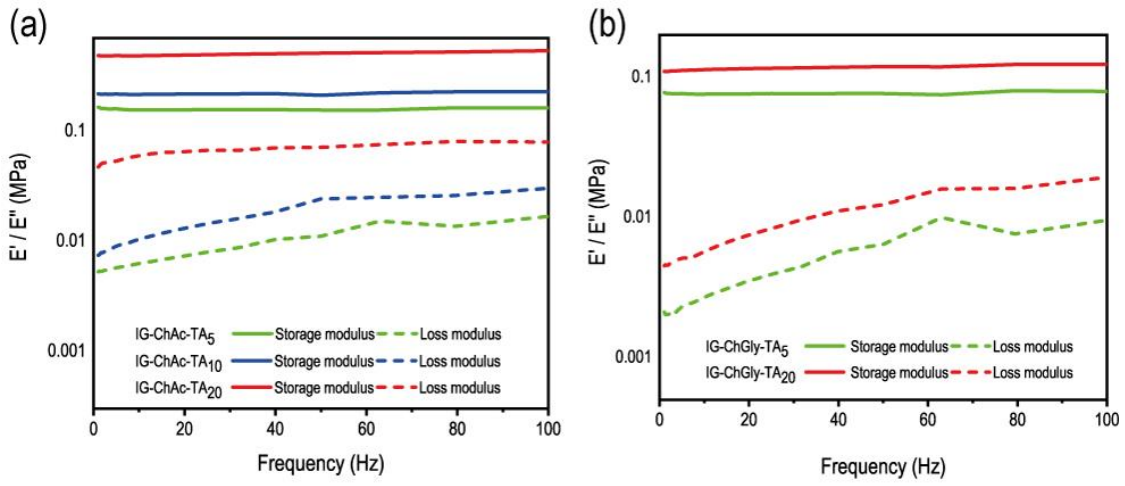

Figure 4. DMTA analysis as a function of the frequency of IG-ChGAc iongels with 5, 10, and 20 wt% of TA (a); and IG-ChGly iongels with 5 and 20 wt% of TA (b).

Thermogravimetric analyses (TGA) were performed to study the temperature range in which the iongels are stable. The TGA profiles obtained are shown in Figure 5 and Figure S8 (SI). The

iongels present good thermal stability, with a temperature of decomposition (T_d) (as the inflection point) between 180 - 220 °C, which agrees with the decomposition patterns of the ILs since both gelatin and TA have higher T_d.[43] The iongels made of [Ch][Ac] IL presented the lowest T_d, while the ones prepared with the [Ch][Lac] IL showed the highest T_d. This can be explained by the different structures (Figure 1.d) of the ILs: the higher their molecular weight, the higher their thermal stability,[44] which can result in higher decomposition temperatures for the respective iongels. The weight loss at around 100 °C is attributed to the evaporation of water. When the iongels reach the equilibrium with the ambient conditions, the final water content is less than 20 wt% (as opposed to the initial content, which is more than 40 %wt), which is mainly a consequence of the hygroscopic nature of these ILs. Although the water remaining within the iongel structure will evaporate at high temperatures, the ionic conduction capacity of the iongels is not affected (unlike hydrogels, which lose all their ionic conductivity properties when dried), as the ILs have negligible vapor pressure and decomposition temperatures over 150 °C.

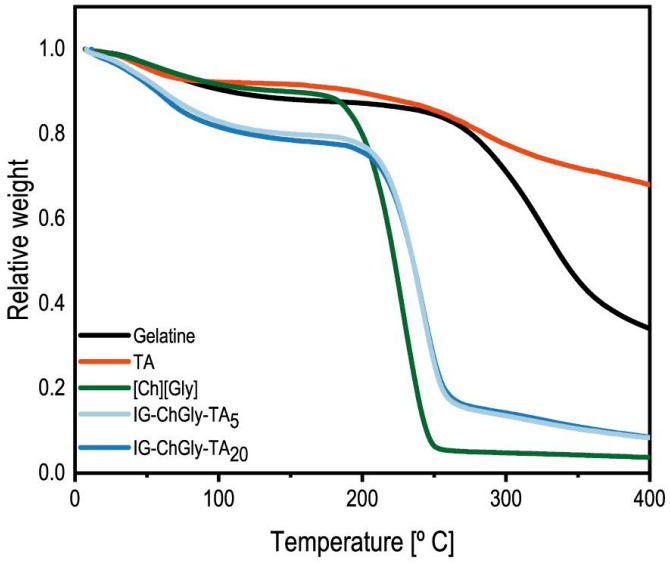

Figure 5. TGA analysis for gelatin, TA. [Ch][Lac] IL, IG-ChLac-TA$_5$ and IG-ChLac-TA$_{20}$.

Iongels for bioelectronic applications are generally required to be flexible and elastic materials. Therefore, the mechanical properties of the iongels were studied by both tensile and compression tests. As a result of the DMTA analyses, E' is higher than E'' for all samples,

indicating a predominant elastic behavior. Compression results can further confirm this theory if the sample returns to its original shape and dimensions after each cycle of compression. The results of the compression test performed with the IG-ChAc-TA_5 sample are shown in Figure 6.a, where each curve corresponds to a full cycle of compression. In a compression cycle, the tip of the probe approaches the sample until making the first contact (point a) and the first value of strain is measured. The tip continues to go down until the full cycle of compression is finished (point b). Then, the tip of the probe moves to its original position, allowing the sample to recover its original shape. As seen in Figure 6.a, all cycles performed started by the probe contacting the sample at the same point. This means that the iongel returned to its initial dimension after being compressed, demonstrating its elastic behavior at high deformation range. All the iongel samples revealed similar performances.

The results of the tensile tests are presented in Figure 6.b. Surprisingly, the iongels containing different amounts of TA do not significantly show different Young's modulus (as seen by the similar slope in the curves corresponding to the same IL). It seems that the mechanical resistance of the iongels is governed by the IL employed. Tensile tests also revealed that all the prepared iongel materials present elastic behavior and might stretch up to at least 225% of their original length (see Table S.2 of the SI for further details).

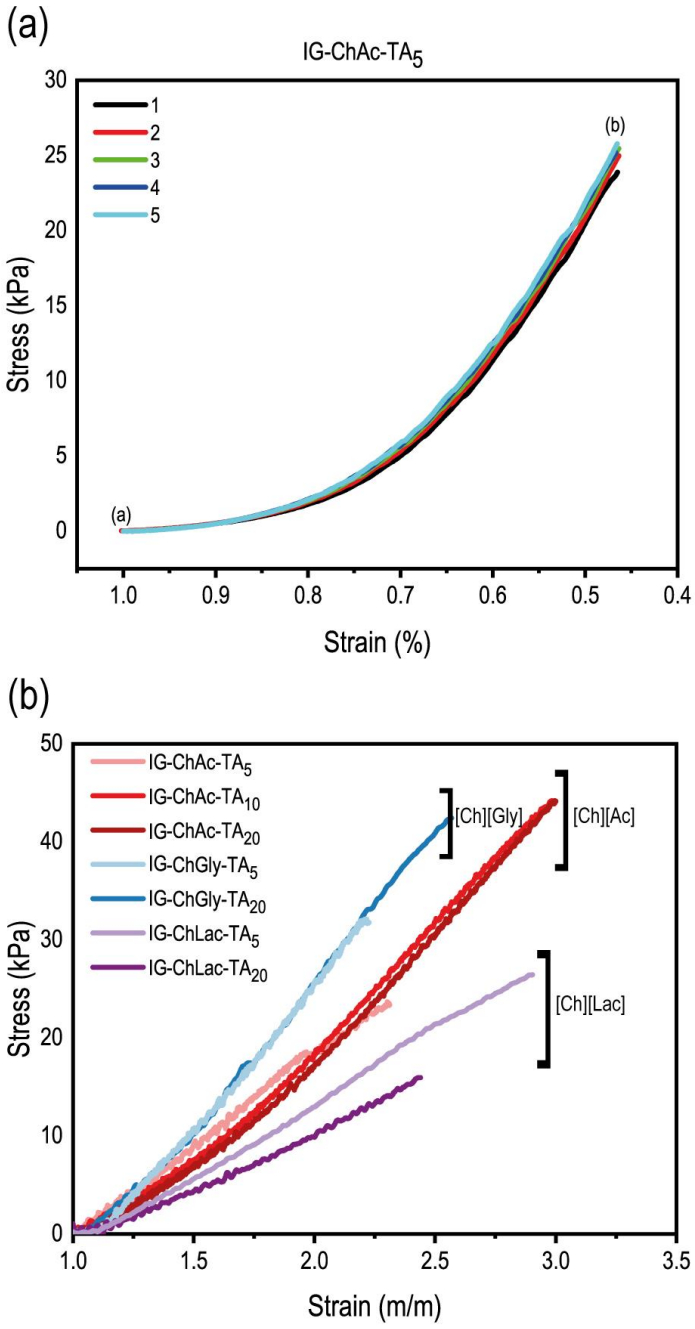

Figure 6. Compression test cycles for GI-ChAc-TA$_5$ (a). Tensile test for gelatin-TA-[Ch][Ac] iongels with 5, 10 and 20 wt% of TA, for Gelatin-TA-[Ch][Gly] iongels with 5 and 20 wt% of TA and for Gelatin-TA-[Ch][Lac] iongels with 5 and 20 wt% of TA (b).

To analyze the microstructure of the surface of the iongels SEM was performed. As it can be seen in Figure 7, even when water was previously evaporated, the presence of the IL within the structure makes it hard to see the polymer network of the iongel. This observation is in

accordance with what has been previously reported for supramolecular PVA/phenolic-based iongels.[21]

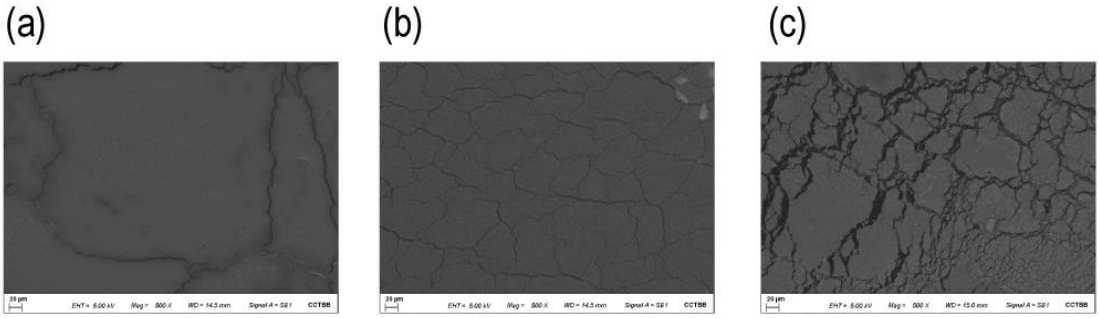

Figure 7. SEM images for IG-ChAc-TA$_{20}$ (a), IG-ChGly-TA$_{20}$ (b) and IG-ChLac-TA$_{20}$ (c) at 500x magnification.

It is well-recognized that ionic conductivity (σ) is one of the most interesting characteristics of iongels, which is given by the presence of ILs.[16] The ionic conductivity of the prepared iongels is shown in Figure 8, in the temperature range between 20 and 60 °C. The ionic conductivity of iongels follows the expected tendency, where ionic mobility is increased with temperature.[16] All the iongels presented high ionic conductivity values at room temperature from 0.003 S*cm^{-1} up to 0.015 S*cm^{-1}. These values are in the high range as those obtained for previous iongels reported in the literature for bioelectronic applications.[20,28,45] The IG-ChAc-TA$_{20}$ iongel exhibited the highest conductivity value. It should also be noted that the amount of TA incorporated into the iongels does not significantly affect the ionic conductivity.

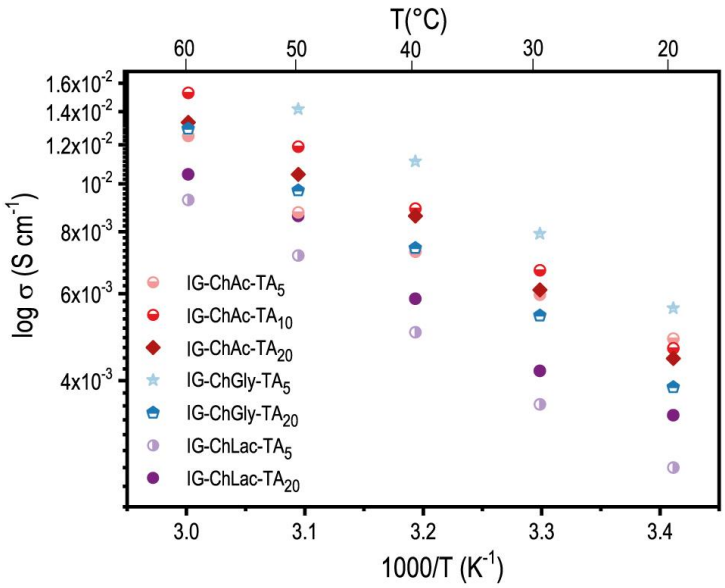

Figure 8. Ionic conductivity of iongels with different ILs and wt% of TA.

As indicated in the introduction, the biocompatibility of iongels must be ensured for bioelectronic applications which involve direct contact the human body. For this reason, the biocompatibility of the iongel materials was investigated by cytotoxicity analysis using NIH/3T3 fibroblasts. Pictures of NIH/3T3 cells incubated with 100% of different iongels extracts revealed a viable adherent monolayer. The morphology of NIH/3T3 was similar to the proliferation control. As expected, the only exception was rubber (toxicity control), which exhibited mainly dead cells (Figure 9.a). The cytotoxicity assays revealed that the relative viability of cells incubated with 100% iongels extracts was significantly higher compared with the cytotoxicity control (rubber), which exhibited a value lower than 10% (ANOVA, $p < 0.05$). More than 70% of cell viability was retained when 100% of iongels extracts were incubated with the cells. Only in the case of IG-ChGly-TA20 iongel, the relative viability was 63%. The analysis of iongels extracts at percentages equal to or lower than 10% revealed no cytotoxic effect since the relative viabilities were higher than 90% (Fig.12b). These results confirmed that iongels extracts are well tolerated by murine fibroblasts.

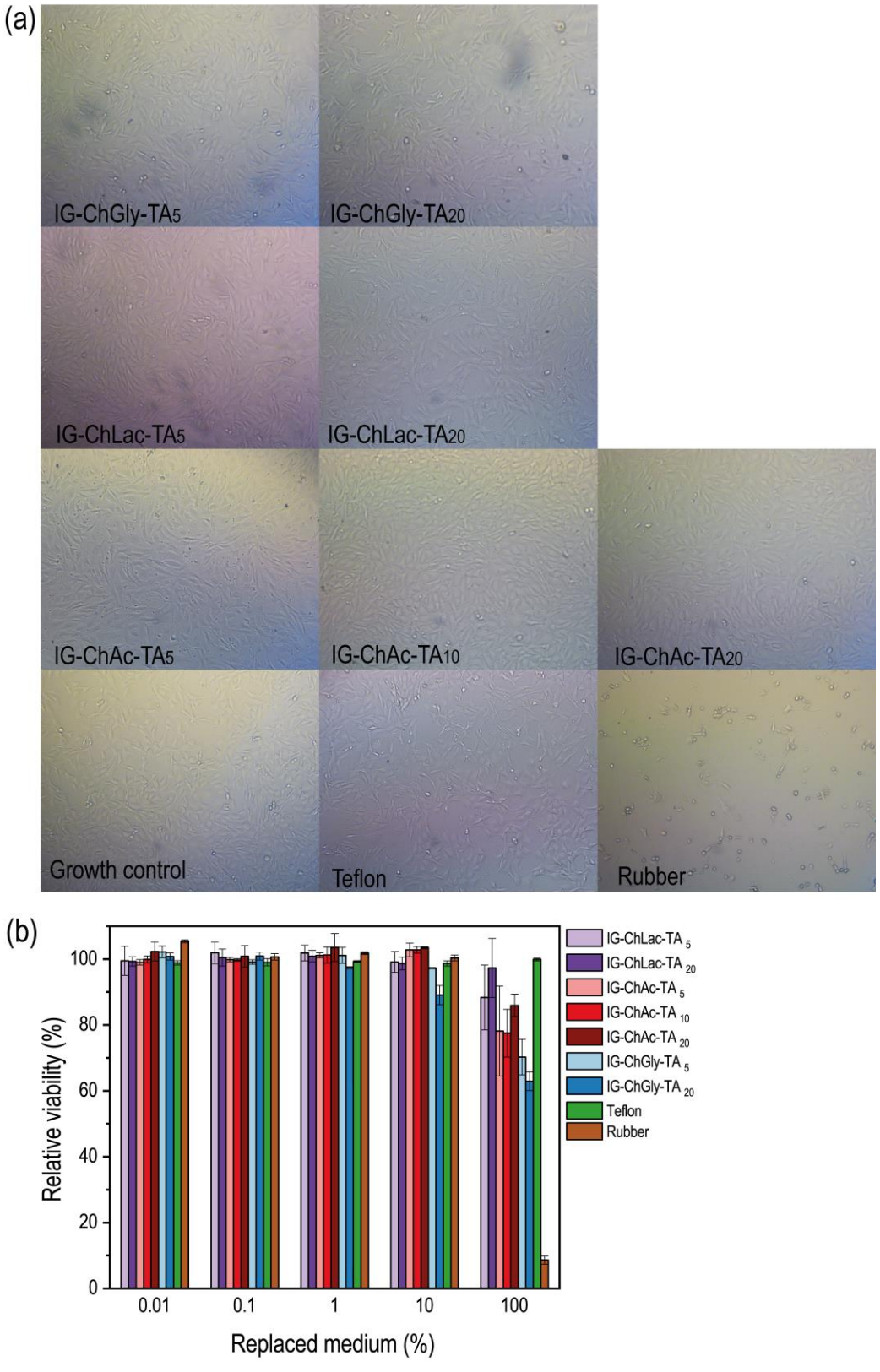

Figure 9. Microscopy of NIH/3T3 cells incubated with 100% iongels extracts (a) and relative viability of NIH/3T3 cells after exposure to 100, 10, 1, 0.1, and 0.01% of IG extracts (b).

The cutaneous electrodes currently used in diverse electrophysiological procedures, such as electroencephalography or electromyography (EMG), present several limitations for long-term recording.[8,16] The standard electrodes employed require the use of an aqueous electrolyte solution or gel to decrease the impedance in the electrode/skin interface.[46] Over time, these electrolyte gels solutions dehydrate by causing a decrease in the recorded signals. Therefore, electrodes employing iongels instead of hydrogels can be highly beneficial for accurate long-term recordings. Impedance spectra of the iongel electrodes can be seen in Figure S9 of SI. The results are similar to the commercial medical electrode. Also, it is clear from all the experiments that it is possible to acquire human motion signals. The iongel materials present a sufficiently low impedance to be used in bioelectronic applications.

Then, EMG recording and muscle stimulation experiments were performed to evaluate the potential of the gelatin-TA iongels as soft ionic conducting materials for bioelectronics. Considering that the ionic conductivity behavior is similar, it is expected that the recordings would not vastly differ between the iongel samples. The iongels were sufficiently adhesive and conductive to measure and fix the electrodes to the skin without requiring the use of tape. The EMGs were recorded for two different muscle activities, where either the muscle contractions were self-performed by the patient, or generated by an external stimulation. Figure 10 shows the recordings using both iongel-based electrodes and a medical degree electrode as a reference while the patient applied self-performed long muscle contractions. Although the measurements of short-time periods are presented, a higher number of contraction and relaxation periods were recorded to guarantee the experimental reproducibility. Contraction periods are indicated by colored backgrounds, while the white backgrounds show muscle relaxation. Although the medical electrode recordings showed higher intensity than IG-ChAc-TA_{20} and IG-ChLac-TA_{20} iongel-based electrodes, a noisier signal was also observed. The small observed differences in the signal shape are a consequence of the variation in the voluntary

movements of the patient. Additionally, EMG recordings involving iongels with the same IL ([Ch][Ac]) and different TA concentrations are compared in Figure S10. As it can be seen, TA concentration does not significantly affect the recordings of iongel-based electrodes. More importantly, the intensity obtained with the iongels proposed in this work was sufficient to record the muscle activity and obtain a better resolution and identification between muscle contraction and relaxation periods.

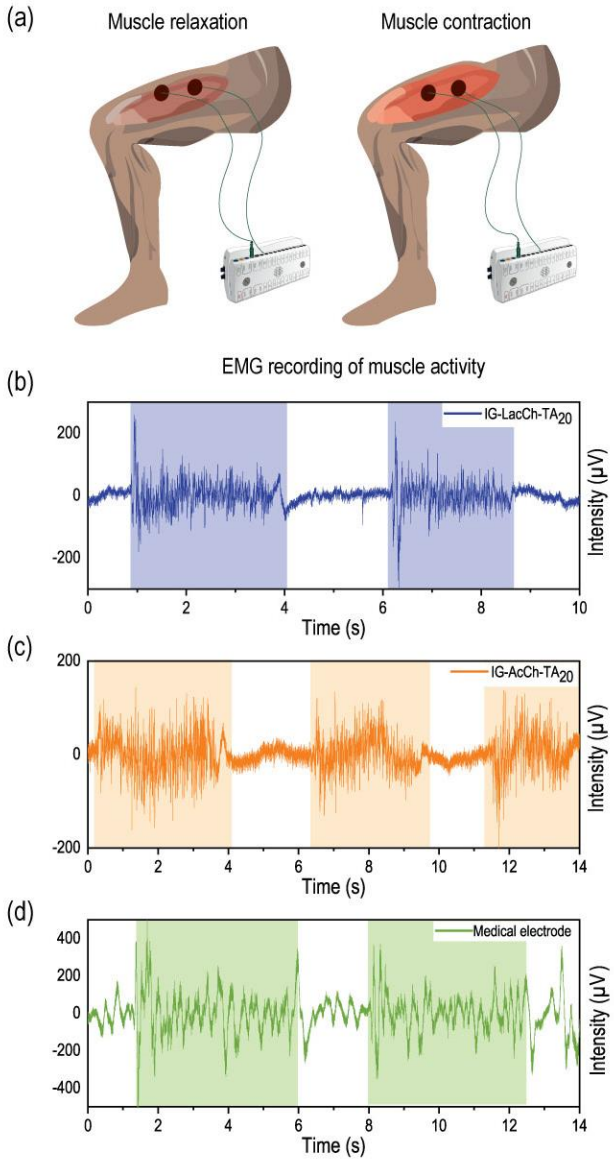

Figure 10. EMGs recording with long self-induced muscle contractions on the quadriceps. Scheme of the assay (a), and EMG recording for electrodes with IG-ChLac-TA$_{20}$ (b), IG-ChAc-TA$_{20}$ (c), and a medical standard electrode (d).

In addition, medical electrodes were used to induce muscle activity in the patient's quadricep, and that activity was measured both with iongel-based electrodes and medical electrodes. Results are depicted in Figure 11. As with self-patient muscle contractions, electrodes containing the iongels allowed a clear and correct signal of the EMGs. Further experiments of muscle stimulation were performed on a patient's quadriceps with electrodes containing the iongels (Video S.1 of the SI). The muscle stimulation was visible in plain sight. These experiments show that the proposed gelatin-TA iongels are capable of both stimulating and recording muscle activity and thus, have potential application for bioelectronic devices in electrophysiological procedures.

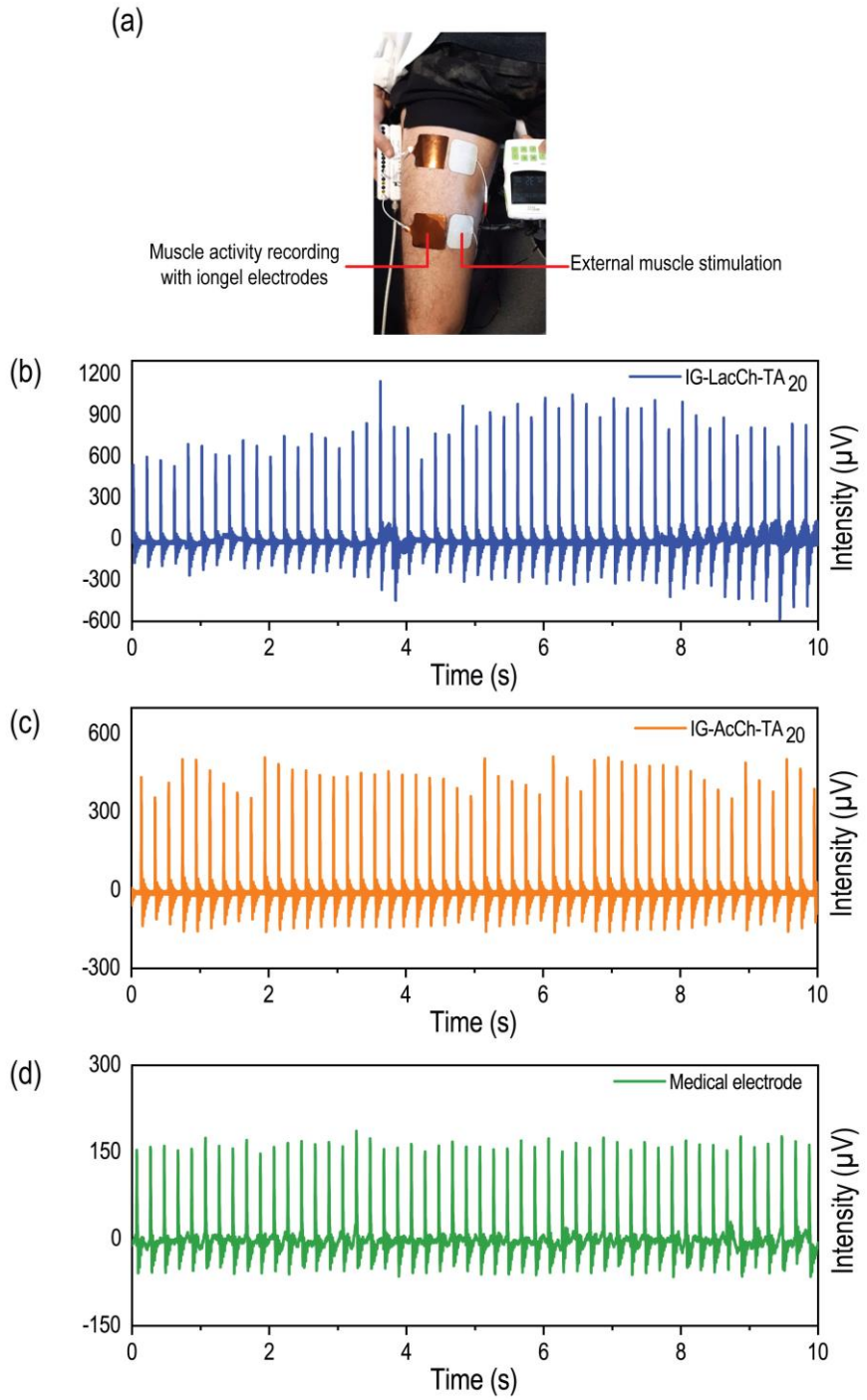

Figure 9. EMGs recordings with standard-medical-electrode-induced muscle contraction. Picture of the assay (a), and EMG recording for electrodes containing IG-ChLac-TA$_{20}$ (b), electrodes containing IG-ChAc-TA$_{20}$ (c), and a medical standard electrode (d).

It was our interest to further observe the use of iongels-based electrodes in other forms of human motion. Figure S11 shows EMGs for IG-ChAc-TA_{10} and medical electrodes for self-induced biceps motions. The response is similar to that was found for EMGs of quadriceps motions. Furthermore, ECGs measurements were performed for IG-ChAc-TA_5 and IG-ChAc-TA_{10} iongel samples. Figure 12 depicts the results, where it could be observed that the iongels based ECG electrodes can well capture the heart's electrical activity.

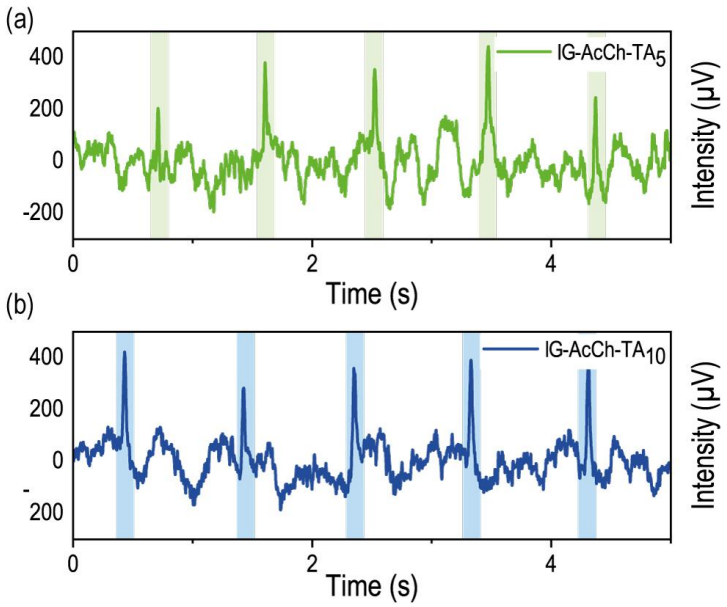

Figure 10. ECG recording for electrodes with IG-ChAc-TA_5 (a), IG-ChAc-TA_{10} (b).

Conclusions

This work proposes iongel materials fully composed of biocompatible components, namely tannic acid (TA), gelatin protein matrix and cholinium carboxylate ILs. The iongel network structure is formed by a dual bonding system, where both chemical bonds (by the reaction of the gelatin's amines with the polyphenol units) and physical interactions (between the gelatin and TA) are present. The resulting iongels are flexible and elastic showing Young's modulus ranging from 11.3 to 28.9 kPa. The biocompatible iongel materials exhibited high ionic conductivity values (between 0.003 $S*cm^{-1}$ and up to 0.015 $S*cm^{-1}$) and showed excellent

performance when used as electrodes in both electromyography and electrocardiogram measurements as well as in muscle stimulation experiments. Interestingly, these iongels presented better resolution than the standard medical electrode, allowing for better identification of the muscle signals. Overall, the gelatin-TA based iongels here proposed unveiled good mechanical and ionic conductivity properties, as well as great suitability to be employed as body sensors in bioelectronic devices.

Supporting Information

Schematic of EIS measurement and EMG assay for self-performed muscle activity, DMTA analysis as a function of the frequency of IG-ChGly iongels, DMTA analysis as a function of the temperature of IG-ChAc, IG-ChLac, and IG-ChLac iongels, pictures of IG-ChAc-TA20 synthesized under nitrogen and oxygen saturated atmospheres, DMTA analysis of IG-ChAc-TA20 synthesized under nitrogen atmosphere and normal conditions, UV spectra for IG-ChAc-TA20, TA, gelatin, and [Ch][Ac], elastic modulus (E') values at different temperatures, picture of IG-ChAc-TA20 iongels after 24 h of immersion in PBS, TGA analysis for all iongels synthesized, impedance spectrum as a function of frequency, tensile tests parameters, EMGs recording with long self-induced muscle contractions on the quadriceps for electrodes with IG-ChAc-TA5, IG-ChAc-TA10, and IG-ChAc-TA20, EMGs recording with long self-induced muscle contractions on the bicep for the electrode with IG-ChAc-TA10 and a medical standard electrode, video of muscle stimulation performed with IG-ChAc-TA20 electrodes.

Acknowledgments

This work was supported by Marie Sklodowska-Curie Research and Innovation Staff Exchanges (RISE) under grant agreement No 823989 "IONBIKE". The Group of Polymer of INTEC acknowledges the financial support from CONICET (PIP 11220200101353CO), ANPCyT (PICT-

2019-01265), and the National University of the Litoral (C.A.I.+D 50620190100117LI). Liliana C. Tomé is grateful to FCT (Fundação para a Ciência e a Tecnologia) in Portugal for her research contract under Scientific Employment Stimulus (2020.01555.CEECIND). Associate Laboratory for Green Chemistry – LAQV also acknowledges the financial support from FCT/MCTES (UIDB/50006/2020 and UIDP/50006/2020).

References

(1) Tomé, L. C.; Mecerreyes, D. Emerging Ionic Soft Materials Based on Deep Eutectic Solvents. *J. Phys. Chem. B* **2020**, *124* (39), 8465–8478. https://doi.org/10.1021/acs.jpcb.0c04769.

(2) Yu, C.; Duan, Z.; Yuan, P.; Li, Y.; Su, Y.; Zhang, X.; Pan, Y.; Dai, L. L.; Nuzzo, R. G.; Huang, Y.; Jiang, H.; Rogers, J. A. Electronically Programmable, Reversible Shape Change in Two- and Three-Dimensional Hydrogel Structures. *Adv. Mater.* **2013**, *25* (11), 1541–1546. https://doi.org/10.1002/adma.201204180.

(3) Deng, Z.; Wang, H.; Ma, P. X.; Guo, B. Self-Healing Conductive Hydrogels: Preparation, Properties and Applications. *Nanoscale* **2020**, *12* (3), 1224–1246. https://doi.org/10.1039/c9nr09283h.

(4) Deng, Z.; Hu, T.; Lei, Q.; He, J.; Ma, P. X.; Guo, B. Stimuli-Responsive Conductive Nanocomposite Hydrogels with High Stretchability, Self-Healing, Adhesiveness, and 3D Printability for Human Motion Sensing. *ACS Appl. Mater. Interfaces* **2019**, *11* (7), 6796–6808. https://doi.org/10.1021/acsami.8b20178.

(5) Deng, Z.; Guo, Y.; Zhao, X.; Ma, P. X.; Guo, B. Multifunctional Stimuli-Responsive Hydrogels with Self-Healing, High Conductivity, and Rapid Recovery through Host-Guest Interactions. *Chem. Mater.* **2018**, *30* (5), 1729–1742.

https://doi.org/10.1021/acs.chemmater.8b00008.

(6) Yang, Q.; Hu, Z.; Rogers, J. A. Functional Hydrogel Interface Materials for Advanced Bioelectronic Devices. *Accounts Mater. Res.* **2021**, *2* (11), 1010–1023. https://doi.org/10.1021/accountsmr.1c00142.

(7) Yu, C.; Guo, H.; Cui, K.; Li, X.; Ye, Y. N.; Kurokawa, T.; Gong, J. P. Hydrogels as Dynamic Memory with Forgetting Ability. *Proc. Natl. Acad. Sci. U. S. A.* **2020**, *117* (32), 18962–18968. https://doi.org/10.1073/pnas.2006842117.

(8) Huang, S.; Liu, Y.; Zhao, Y.; Ren, Z.; Guo, C. F. Flexible Electronics: Stretchable Electrodes and Their Future. *Adv. Funct. Mater.* **2019**, *29* (6), 1–15. https://doi.org/10.1002/adfm.201805924.

(9) Wang, H.; Wang, Z.; Yang, J.; Xu, C.; Zhang, Q.; Peng, Z. Ionic Gels and Their Applications in Stretchable Electronics. **2018**, *1800246*, 1–17. https://doi.org/10.1002/marc.201800246.

(10) Qin, H.; Owyeung, R. E.; Sonkusale, S. R.; Panzer, M. J. Highly Stretchable and Nonvolatile Gelatin-Supported Deep Eutectic Solvent Gel Electrolyte-Based Ionic Skins for Strain and Pressure Sensing. *J. Mater. Chem. C* **2019**, *7* (3), 601–608. https://doi.org/10.1039/c8tc05918g.

(11) Cao, Z.; Liu, H.; Jiang, L. Transparent, Mechanically Robust, and Ultrastable Ionogels Enabled by Hydrogen Bonding between Elastomers and Ionic Liquids. *Mater. Horizons* **2020**, *7* (3), 912–918. https://doi.org/10.1039/c9mh01699f.

(12) Cao, Y.; Tan, Y. J.; Li, S.; Lee, W. W.; Guo, H.; Cai, Y.; Wang, C.; Tee, B. C. K. Self-Healing Electronic Skins for Aquatic Environments. *Nat. Electron.* **2019**, *2* (2), 75–82. https://doi.org/10.1038/s41928-019-0206-5.

(13) Hong, S.; Yuan, Y.; Liu, C.; Chen, W.; Chen, L.; Lian, H.; Liimatainen, H. A Stretchable and Compressible Ion Gel Based on a Deep Eutectic Solvent Applied as a Strain Sensor and Electrolyte for Supercapacitors. *J. Mater. Chem. C* **2020**, *8* (2), 550–560. https://doi.org/10.1039/c9tc05913j.

(14) Leleux, P.; Johnson, C.; Strakosas, X.; Rivnay, J.; Hervé, T.; Owens, R. M.; Malliaras, G. G. Ionic Liquid Gel-Assisted Electrodes for Long-Term Cutaneous Recordings. *Adv. Healthc. Mater.* **2014**, *3* (9), 1377–1380. https://doi.org/10.1002/adhm.201300614.

(15) Yuen, A. Y.; Porcarelli, L.; Aguirresarobe, R. H.; Sanchez-Sanchez, A.; del Agua, I.; Ismailov, U.; Malliaras, G. G.; Mecerreyes, D.; Ismailova, E.; Sardon, H. Biodegradable Polycarbonate Iongels for Electrophysiology Measurements. *Polymers (Basel).* **2018**, *10* (9). https://doi.org/10.3390/polym10090989.

(16) Isik, M.; Lonjaret, T.; Sardon, H.; Marcilla, R.; Herve, T.; Malliaras, G. G.; Ismailova, E.; Mecerreyes, D. Cholinium-Based Ion Gels as Solid Electrolytes for Long-Term Cutaneous Electrophysiology. *J. Mater. Chem. C* **2015**, *3* (34), 8942–8948. https://doi.org/10.1039/c5tc01888a.

(17) Kunz, W.; Maurer, E.; Klein, R.; Touraud, D.; Rengstl, D.; Harrar, A.; Dengler, S.; Zech, O. Low Toxic Ionic Liquids, Liquid Catanionics, and Ionic Liquid Microemulsions. *J. Dispers. Sci. Technol.* **2011**, *32* (12), 1694–1699. https://doi.org/10.1080/01932691.2011.616109.

(18) Cornellas, A.; Perez, L.; Comelles, F.; Ribosa, I.; Manresa, A.; Garcia, T. T. Self-Aggregation and Antimicrobial Activity of Imidazolium and Pyridinium Based Ionic Liquids in Aqueous Solution. *J. Colloid Interface Sci.* **2011**, *355* (1), 164–171. https://doi.org/10.1016/j.jcis.2010.11.063.

(19) Petkovic, M.; Ferguson, J. L.; Gunaratne, H. Q. N.; Ferreira, R.; Leitão, M. C.; Seddon, K.

R.; Rebelo, L. P. N.; Pereira, C. S. Novel Biocompatible Cholinium-Based Ionic Liquids—Toxicity and Biodegradability. *Green Chem.* **2010**, *12* (4), 643–664. https://doi.org/10.1039/b922247b.

(20) Luque, G. C.; Picchio, M. L.; Martins, A. P. S.; Dominguez-Alfaro, A.; Ramos, N.; del Agua, I.; Marchiori, B.; Mecerreyes, D.; Minari, R. J.; Tomé, L. C. 3D Printable and Biocompatible Iongels for Body Sensor Applications. *Adv. Electron. Mater.* **2021**, *2100178*, 2100178. https://doi.org/10.1002/aelm.202100178.

(21) Luque, G. C.; Picchio, M. L.; Martins, A. P. S.; Dominguez-Alfaro, A.; Tomé, L. C.; Mecerreyes, D.; Minari, R. J. Elastic and Thermoreversible Iongels by Supramolecular PVA/Phenol Interactions. *Macromol. Biosci.* **2020**, *2000119*, 1–8. https://doi.org/10.1002/mabi.202000119.

(22) Euti, E. M.; Wolfel, A.; Picchio, M. L.; Romero, M. R.; Martinelli, M.; Minari, R. J.; Igarzabal, C. I. A. Controlled Thermoreversible Formation of Supramolecular Hydrogels Based on Poly(Vinyl Alcohol) and Natural Phenolic Compounds. *Macromol. Rapid Commun.* **2019**, *40* (18), 1900217. https://doi.org/10.1002/marc.201900217.

(23) Fang, H.; Wang, J.; Li, L.; Xu, L.; Wu, Y.; Wang, Y.; Fei, X.; Tian, J.; Li, Y. A Novel High-Strength Poly(Ionic Liquid)/PVA Hydrogel Dressing for Antibacterial Applications. *Chem. Eng. J.* **2019**, *365* (February), 153–164. https://doi.org/10.1016/j.cej.2019.02.030.

(24) Takada, A.; Kadokawa, J. I. Fabrication and Characterization of Polysaccharide Ion Gels with Ionic Liquids and Their Further Conversion into Value-Added Sustainable Materials. *Biomolecules* **2015**, *5* (1), 244–262. https://doi.org/10.3390/biom5010244.

(25) Kadokawa, J. ichi; Murakami, M. aki; Kaneko, Y. A Facile Preparation of Gel Materials from a Solution of Cellulose in Ionic Liquid. *Carbohydr. Res.* **2008**, *343* (4), 769–772. https://doi.org/10.1016/j.carres.2008.01.017.

(26) Isik, M.; Gracia, R.; Kollnus, L. C.; Tomé, L. C.; Marrucho, I. M.; Mecerreyes, D. Cholinium-Based Poly(Ionic Liquid)s: Synthesis, Characterization, and Application as Biocompatible Ion Gels and Cellulose Coatings. *ACS Macro Lett.* **2013**, *2* (11), 975–979. https://doi.org/10.1021/mz400451g.

(27) Plappert, S. F.; Nedelec, J. M.; Rennhofer, H.; Lichtenegger, H. C.; Bernstorff, S.; Liebner, F. W. Self-Assembly of Cellulose in Super-Cooled Ionic Liquid under the Impact of Decelerated Antisolvent Infusion: An Approach toward Anisotropic Gels and Aerogels. *Biomacromolecules* **2018**, *19* (11), 4411–4422. https://doi.org/10.1021/acs.biomac.8b01278.

(28) Del Agua, I.; Mantione, D.; Casado, N.; Sanchez-Sanchez, A.; Malliaras, G. G.; Mecerreyes, D. Conducting Polymer Iongels Based on PEDOT and Guar Gum. *ACS Macro Lett.* **2017**, *6* (4), 473–478. https://doi.org/10.1021/acsmacrolett.7b00104.

(29) Rawat, K.; Pathak, J.; Bohidar, H. B. Effect of Solvent Hydrophobicity on Gelation Kinetics and Phase Diagram of Gelatin Ionogels. *Soft Matter* **2014**, *10* (6), 862–872. https://doi.org/10.1039/c3sm52701h.

(30) Vidinha, P.; Lourenço, N. M. T.; Pinheiro, C.; Brás, A. R.; Carvalho, T.; Santos-Silva, T.; Mukhopadhyay, A.; Romão, M. J.; Parola, J.; Dionisio, M.; Cabral, J. M. S.; Afonso, C. A. M.; Barreiros, S. Ion Jelly: A Tailor-Made Conducting Material for Smart Electrochemical Devices. *Chem. Commun.* **2008**, No. 44, 5842–5844. https://doi.org/10.1039/b811647d.

(31) Muhoza, B.; Xia, S.; Zhang, X. Gelatin and High Methyl Pectin Coacervates Crosslinked with Tannic Acid: The Characterization, Rheological Properties, and Application for Peppermint Oil Microencapsulation. *Food Hydrocoll.* **2019**, *97* (March), 105174. https://doi.org/10.1016/j.foodhyd.2019.105174.

(32) Gerrard, J. A.; Brown, P. K.; Fayle, S. E. Maillard Crosslinking of Food Proteins I: The

Reaction of Glutaraldehyde, Formaldehyde and Glyceraldehyde with Ribonuclease. *Food Chem.* **2002**, *79* (3), 343–349. https://doi.org/10.1016/S0308-8146(02)00174-7.

(33) Gerrard, J. A.; Brown, P. K.; Fayle, S. E. Maillard Crosslinking of Food Proteins II: The Reactions of Glutaraldehyde, Formaldehyde and Glyceraldehyde with Wheat Proteins in Vitro and in Situ. *Food Chem.* **2003**, *80* (1), 35–43. https://doi.org/10.1016/S0308-8146(02)00232-7.

(34) Gerrard, J. A.; Brown, P. K. Protein Cross-Linking in Food: Mechanisms, Consequences, Applications. *Int. Congr. Ser.* **2002**, *1245* (C), 211–215. https://doi.org/10.1016/S0531-5131(02)00910-X.

(35) Siebert, K. J. Effects of Protein-Polyphenol Interactions on Beverage Haze, Stabilization, and Analysis. *J. Agric. Food Chem.* **1999**, *47* (2), 353–362. https://doi.org/10.1021/jf980703o.

(36) Zhang, X.; Do, M. D.; Casey, P.; Sulistio, A.; Qiao, G. G.; Lundin, L.; Lillford, P.; Kosaraju, S. Chemical Cross-Linking Gelatin with Natural Phenolic Compounds as Studied by High-Resolution NMR Spectroscopy. *Biomacromolecules* **2010**, *11* (4), 1125–1132. https://doi.org/10.1021/bm1001284.

(37) Singh, H. Modification of Food Proteins by Covalent Crosslinking. *Trends Food Sci. Technol.* **1991**, *2* (C), 196–200. https://doi.org/10.1016/0924-2244(91)90683-A.

(38) Picchio, M. L.; Linck, Y. G.; Monti, G. A.; Gugliotta, L. M.; Minari, R. J.; Alvarez Igarzabal, C. I. Casein Films Crosslinked by Tannic Acid for Food Packaging Applications. *Food Hydrocoll.* **2018**, *84*, 424–434. https://doi.org/10.1016/j.foodhyd.2018.06.028.

(39) Miranda, R. B.; Fidel, S. R.; Boller, M. A. A. L929 Cell Response to Root Perforation Repair Cements: An in Vitro Cytotoxicity Assay. *Braz. Dent. J.* **2009**, *20* (1), 22–26.

https://doi.org/10.1590/S0103-64402009000100003.

(40) del Agua, I.; Mantione, D.; Ismailov, U.; Sanchez-Sanchez, A.; Aramburu, N.; Malliaras, G. G.; Mecerreyes, D.; Ismailova, E. DVS-Crosslinked PEDOT:PSS Free-Standing and Textile Electrodes toward Wearable Health Monitoring. *Adv. Mater. Technol.* **2018**, *3* (10), 1–8. https://doi.org/10.1002/admt.201700322.

(41) Strauss, G.; Gibson, S. M. Plant Phenolics as Cross-Linkers of Gelatin Gels and Gelatin-Based Coacervates for Use as Food Ingredients. *Food Hydrocoll.* **2004**, *18* (1), 81–89. https://doi.org/10.1016/S0268-005X(03)00045-6.

(42) Anvari, M.; Chung, D. Dynamic Rheological and Structural Characterization of Fish Gelatin - Gum Arabic Coacervate Gels Cross-Linked by Tannic Acid. *Food Hydrocoll.* **2016**, *60*, 516–524. https://doi.org/10.1016/j.foodhyd.2016.04.028.

(43) Dbira, S.; Bensalah, N.; Zagho, M. M.; Ennahaoui, M.; Bedoui, A. Oxidative Degradation of Tannic Acid in Aqueous Solution by UV/S2O82- and UV/H2O2/Fe2+ Processes: A Comparative Study. *Appl. Sci.* **2019**, *9* (1). https://doi.org/10.3390/app9010156.

(44) Maton, C.; De Vos, N.; Stevens, C. V. Ionic Liquid Thermal Stabilities: Decomposition Mechanisms and Analysis Tools. *Chem. Soc. Rev.* **2013**, *42* (13), 5963–5977. https://doi.org/10.1039/c3cs60071h.

(45) Li, Z.; Wang, J.; Hu, R.; Lv, C.; Zheng, J. A Highly Ionic Conductive, Healable, and Adhesive Polysiloxane-Supported Ionogel. *Macromol. Rapid Commun.* **2019**, *40* (7), 1–6. https://doi.org/10.1002/marc.201800776.

(46) Soroudi, A.; Hernández, N.; Wipenmyr, J.; Nierstrasz, V. Surface Modification of Textile Electrodes to Improve Electrocardiography Signals in Wearable Smart Garment. *J. Mater. Sci. Mater. Electron.* **2019**, *30* (17), 16666–16675. https://doi.org/10.1007/s10854-019-

02047-9.

For Table of Contents Use Only

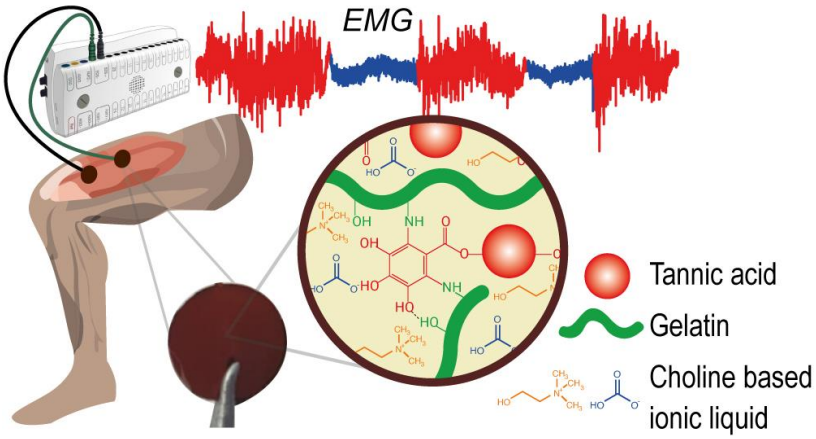

Gelatin and tannic acid-based iongels for muscle activity recording and stimulation electrodes

Ana Aguzin, Gisela C. Luque, Ludmila I. Ronco, Isabel del Agua, Gregorio Guzmán-González, Bastien Marchiori, Agustina Gugliotta, Liliana C. Tomé, Luis M. Gugliotta, David Mecerreyes, and Roque J. Minari